π phase shift across stripes in a charge density wave system

T. Ying,[1,*] R. T. Scalettar,[2,†] and R. Mondaini[3,‡]
[1]*School of Physics, Harbin Institute of Technology, Harbin 150001, China*
[2]*Department of Physics, University of California, Davis, California 95616, USA*
[3]*Beijing Computational Science Research Center, Beijing 100193, China*

(Received 28 October 2021; revised 4 March 2022; accepted 4 March 2022; published 14 March 2022)

Many strongly correlated materials are characterized by deeply intertwined charge and spin order. Besides their high superconducting transition temperatures, one of the central features of these complex patterns in cuprates is a phase shift which occurs across lines of decreased hole density. That is, when doped away from their antiferromagnetic phase, the additional charge is not distributed uniformly, but rather in "stripes." The sublattices preferentially occupied by up and down spin are reversed across these stripes, a phenomenon referred to as a "π phase shift." Many of the spin-charge patterns, including the π phase shift, are reproduced by density matrix renormalization group and quantum Monte Carlo calculations of simplified tight binding (repulsive Hubbard) models. In this paper we demonstrate that this sublattice reversal is generic by considering the corresponding phenomenon in the attractive Hubbard Hamiltonian, where a charge density wave phase forms at half filling. We introduce charge stripes via an appropriate local chemical potential; measurements of charge correlation across the resulting lines of lowered density reveal a clear π phase.

DOI: 10.1103/PhysRevB.105.115116

I. INTRODUCTION

Inhomogeneous phases are a central feature of strongly correlated materials, and especially of oxide systems [1]. The manganites are one example [2–5]. They have ferromagnetic and antiferromagnetic (AF) states in close proximity in energy, and when a small quenched disorder is included, extended glassy regions emerge in which these phases coexist. This regime is very sensitive to external perturbation, e.g., the application of a small magnetic field, leading to the phenomenon of colossal magnetoresistance. The cuprates are another instance. Here a wide body of experiments, including transport [6], nuclear magnetic resonance [7,8], x-ray scattering [9–11], and scanning tunneling microscopy [12], has indicated that complex patterns of charge and spin develop upon doping [13], and that these inhomogeneous structures are also present in the pairing gaps [11,14], thereby suggesting a possible connection to their high superconducting transition temperatures.

Quite remarkably, many of the intricate details of these structures are reproduced in calculations on simple Hamiltonians, even when the models are translation invariant [15]. Indeed, one of the earliest indications of stripe physics, in which doped holes arrange themselves in linear patterns, came out of mean-field calculations [16–18], predating much of the experimental work. These observations have been confirmed by a wide variety of methods like functional renormalization group [19], the density matrix renormalization group (DMRG) [20–23], exact diagonalization (ED) [24], dynamic mean field theory [25], auxiliary field quantum Monte Carlo (AFQMC) [26–29], infinite projected entangled pair states [30], and density matrix embedding theory [31], all of which treat many-body effects more exactly.

One central feature of these striped phases in the repulsive Hubbard model is their mixed charge and spin character, and in particular, a "π phase shift" in the *spin* correlations which is found to exist across a linear depletion of *charge*: The sublattice which holds the surplus of up spin character on one side of a stripe instead holds a surplus of down spin as the stripe is traversed [32].

In this paper we examine whether such π phase shifts exist in a charge density wave (CDW) phase across a (charge) stripe. That is, we address the question of whether the mixed character of the stripe, and the type of order being established across it, is essential to the existence of a phase shift. We address this question by using determinant quantum Monte Carlo (DQMC) simulations of the *attractive* Hubbard model in which stripes are imposed externally via raising the local site energy along several rows of the lattice. While this method does not establish the spontaneous formation of inhomogeneities, it does allow an exploration of sublattice order reversal. Our focus is not an investigation of specific cuprate physics, but rather to address the general and fundamental issue of the circumstances under which a line of reduced particle density leads to a reversal of the ordered sublattice on either side of the boundary.

However, it is interesting to note that even for cuprate superconductors, typically described in terms of the repulsive Hubbard model and hence with predominantly *magnetic* order, it is observed that the superconducting state also coexists and competes with CDW correlations [33–38]. Indeed, it

*taoying86@hit.edu.cn
†scalettar@physics.ucdavis.edu
‡rmondaini@csrc.ac.cn

has recently been argued that in a certain class of cuprates, phonons play an important role in such CDW formation and lead to strong attractive interactions [39–41]. Similarly, for lithium-deposited graphene [42] or graphite intercalation compounds [43], where superconductivity is phonon mediated, CDW order, forming quasi-one-dimensional patterns of electron-rich regions, is also observed [44]. These examples lend further interest to the question addressed in this paper: Will the π phase shift, observed in the *spin* correlations of the repulsive Hubbard model, also appear in the *charge* degrees of freedom of the attractive Hubbard model?

Significantly, because of the absence of a sign problem [45,46], we are able to examine low temperatures and especially the effect of stripes and the π phase shift on (s-wave) pairing correlations. Addressing such issues is much more challenging in the repulsive Hubbard model [27] because of the sign problem.

Our key results are that the introduction of a charge stripe of sufficient depth does cause the CDW domains on opposite sides of the stripe to develop a π phase shift, so that their high and low density sublattices are interchanged. In this way the structure of the charge order across a density stripe mimics the well-known behavior of the spin order in the repulsive Hubbard model. We also show that this π phase shift appears to be detrimental to pairing order.

This paper is organized as follows. In Sec. II we define the Hamiltonian and correlation functions we will investigate, and give a brief description of the DQMC and ED methodologies. Section III presents our results for charge and pairing correlations, focusing especially on the issue of a π phase shift. Finally, Sec. IV summarizes our conclusions.

II. HAMILTONIAN AND METHODOLOGY

We study a two-dimensional square lattice attractive Hubbard Hamiltonian in which stripes are introduced externally via a raised site energy V_0 on a set of rows of period $\mathcal{P}$, $\mathbf{i} = (i_x, i_y)$ with $\mathrm{mod}(i_y, \mathcal{P}) = 0$:

$$\hat{\mathcal{H}} = -t \sum_{\langle \mathbf{ij} \rangle \sigma} (\hat{c}^\dagger_{\mathbf{i}\sigma} \hat{c}_{\mathbf{j}\sigma} + \hat{c}^\dagger_{\mathbf{j}\sigma} \hat{c}_{\mathbf{i}\sigma}) + U \sum_{\mathbf{i}} \hat{n}_{\mathbf{i}\uparrow} \hat{n}_{\mathbf{i}\downarrow} - \mu \sum_{\mathbf{i}} (\hat{n}_{\mathbf{i}\uparrow} + \hat{n}_{\mathbf{i}\downarrow}) + V_0 \sum_{i_y \in \mathcal{P}} (\hat{n}_{\mathbf{i}\uparrow} + \hat{n}_{\mathbf{i}\downarrow}). \quad (1)$$

We choose $\mathcal{P} = 4$, so that each stripe (row with V_0 term active, blue spheres in Fig. 1) is separated by three rows where the V_0 term is not present (light-colored spheres in Fig. 1). In what follows, the attractive interactions are signaled by the negative value of U used.

Our primary methodology is the DQMC approach [47,48]. We first express the partition function associated with the Hamiltonian of Eq. (1), $\mathcal{Z} = \mathrm{Tr}\, e^{-\beta \hat{\mathcal{H}}}$, as a path integral by discretizing the imaginary time $\beta = L_\tau \Delta\tau$. This allows us to use the Trotter approximation $e^{-\Delta\tau \hat{\mathcal{H}}} \approx e^{-\Delta\tau \hat{\mathcal{K}}} e^{-\Delta\tau \hat{\mathcal{V}}}$, where $\hat{\mathcal{K}}$ and $\hat{\mathcal{V}}$ are the single- and two-particle terms of $\hat{\mathcal{H}}$, respectively. In this work we use $\Delta\tau = 0.1$; an analysis of Trotter errors in observables is given in Appendix B. With $\hat{\mathcal{V}}$ isolated, we can introduce a (discrete) Hubbard-Stratonovich field (HSF) [49] to decouple the interactions. The trace which gives $\mathcal{Z}$ now contains only exponentials of quadratic forms of fermion operators and can be done analytically. The resulting expression for $\mathcal{Z}$ is a sum over the configurations of the HSF, which is done stochastically. The traces over the spin up and spin down electrons are given by the determinants of the same matrix, because (i) both components couple identically to the HSF and (ii) the added stripe energy term does not break SU(2) symmetry. As a result, the product of the determinants is always positive, and hence there is no sign problem [45,46]. We will present results mainly for 8×8 (12×12 and 16×16 lattice results are shown in Appendix C), i.e., linear extent $L = 8$, and supplement the DQMC calculations with ED to confirm and further understand the physics. Our ED calculations, presented in Appendix E, focus on a 2×4 lattice, which has a manageable Hilbert space size yet is large enough to hold a stripe and examine the spin and charge patterns at finite temperature T.

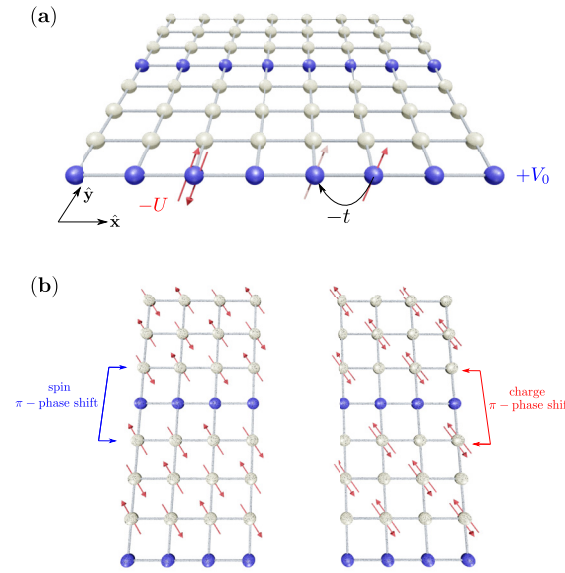

FIG. 1. (a) Illustration of the Hamiltonian in an 8×8 lattice with period $\mathcal{P} = 4$; sites with V_0 active are depicted in blue, whereas the interstripe sites are white. The other relevant parameters, hopping, and attractive interactions are annotated. (b) Schematic cartoon of a π phase shift state for densities $\rho = 0.75$, either in its well-known spin case (left) or the one we explore in this work, with a charge density wave phase when crossing the stripes (right).

For $V_0 \neq 0$, the density is inhomogeneous. We denote by ρ the overall density, averaged over the entire lattice. ρ_{str} is the density on the stripes, the sites with $V_0 \neq 0$, and ρ_{dom} is the density on the domains between the stripes. For $\mathcal{P} = 4$ these are related by $\rho = \frac{1}{4}\rho_{\mathrm{str}} + \frac{3}{4}\rho_{\mathrm{dom}}$.

We focus attention on the equal-time, real-space density-density correlation function

$$c(\mathbf{r}) = \langle (\hat{n}_{\mathbf{i}} - 1)(\hat{n}_{\mathbf{i}+\mathbf{r}} - 1) \rangle \quad (2)$$

between two sites $\mathbf{i}$ and $\mathbf{i} + \mathbf{r}$. Since the V_0 term in Eq. (1) breaks translation invariance in the $\hat{y}$ direction, $c(\mathbf{r})$ will also depend on the fiducial site $\mathbf{i}$. We will typically choose $\mathbf{i}$, as schematically specified in the figures below, to be a site adjacent to a stripe, and select $\mathbf{r}$ to cross the stripe in order to probe the possibility of a π phase shift. The subtraction is a convention, useful for this paper where much of the lattice

has $\langle \hat{n}_{\mathbf{i}} \rangle = 1$, since it then enables a focus on fluctuations away from the average density. In a homogeneous CDW phase, this correlation function is long-ranged, taking positive values for pairs of sites on the same sublattice and negative values for sites on opposite sublattices.

We also examine the equal-time s-wave pairing, and their associated structure factor P_s at $\mathbf{q} = 0$:

$$P_s = \sum_{\mathbf{i},\mathbf{r}} \langle \hat{\Delta}_{\mathbf{i}+\mathbf{r}} \hat{\Delta}_{\mathbf{i}}^{\dagger} \rangle, \quad \hat{\Delta}_{\mathbf{i}}^{\dagger} \equiv \hat{c}_{\mathbf{i}\uparrow}^{\dagger} \hat{c}_{\mathbf{i}\downarrow}^{\dagger}, \tag{3}$$

which signals the formation of a superconducting phase. In the presence of off-diagonal long-range order $\langle \hat{\Delta}_{\mathbf{i}+\mathbf{r}} \hat{\Delta}_{\mathbf{i}}^{\dagger} \rangle$ approaches a nonzero value as $\mathbf{r} \to \infty$, and P_s grows linearly with the lattice size L^2.

In the absence of V_0, and at half filling $\mu = U/2$, the attractive Hubbard model has simultaneous CDW and s-wave order. This enlarged symmetry of possible ordered phases implies that long-range order (LRO) is possible only at $T = 0$ [50,51]. On finite lattices, LRO can be observed as long as the temperature is lowered to a value for which the correlation length ξ exceeds the linear lattice size L. The introduction of stripes ($V_0 \neq 0$) breaks this degeneracy between CDW and pairing. As we will discuss below, the resulting anisotropy favors pairing order, if small in strength, an observation which will be confirmed by our DQMC simulations at small values of V_0. The qualitative argument is similar to that for uniform doping of the attractive Hubbard model [50,51].

III. RESULTS

We first focus separately on the density and pairing correlations, and then comment on how they are related, interpreting the enhancement of pairing order for weak stripes in terms of a particle-hole transformation to the repulsive Hubbard model.

A. Density-density correlations: Demonstration of stripe formation

We begin with DQMC results for the density-density correlations. The central feature of the π phase shift is the interchange of the sublattice ordering pattern across the stripe. A spin (or charge) correlation connecting sites on the *same* sublattice, which would be positive in the absence of a stripe, becomes negative. Likewise, a spin (or charge) correlation connecting sites on the *different* sublattices, which would be negative in the absence of a stripe, becomes positive. The pairs of sites connected by blue and red arrows in the inset of Fig. 2(a) show these two cases.

We perform a set of simulations in which V_0 is increased, gradually forming well-defined stripes of reduced fermion occupation. We simultaneously adjust the global chemical potential μ to keep the density on the sites of the domains between the stripes $\rho_{\text{dom}} = 1$, a value which is optimal for CDW order (other densities are investigated in Appendix D). Figure 2(a) is one of the central results of our paper. It demonstrates that as stripes are introduced, a π phase shift emerges. For the parameters shown, $U = -4t$ and $T = t/10$, the crossover occurs at $V_0 \sim t$.

The corresponding density evolution is shown in Fig. 2(b). The blue curve shows the rapid depletion of fermion occupation on the stripes. At $V_0 \sim t$ where the π phase shift emerges, $\rho_{\text{str}} \sim 0.25$. The black curve shows the overall fermion occupation ρ, which approaches 0.75 in the large-V_0 limit since 1/4 of the sites (the stripes) have been driven to empty with the remaining 3/4 of the sites remaining at unit density. The two curves are not independent, being related, as noted earlier, by $\rho = \frac{3}{4} + \frac{1}{4}\rho_{\text{str}}$; both are shown for clarity, however.

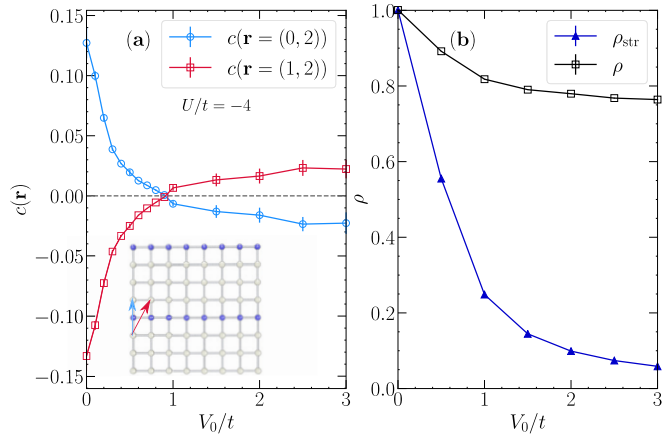

FIG. 2. (a) Density-density correlators $c(\mathbf{r} = (0,2))$ (blue circles, and blue arrow in the inset) and $c(\mathbf{r} = (1,2))$ (red squares, and red arrow in the inset), as functions of stripe strength V_0. The emergence of π phase shift at $V_0 \sim t$ is signaled by the reversal in sign of the correlation functions. (b) The total electron density ρ and the density on the stripe ρ_{str}, as functions of stripe strength V_0. The electron density off stripe ρ_{dom} is fixed to be 1 by adjusting the global chemical potential μ. Here the lattice size is 8×8, the on-site attraction $U = -4t$ is half the noninteracting bandwidth, and the inverse temperature $\beta t = 10$.

If one instead investigates the *repulsive* Hubbard model ($U > 0$), see Appendix A, a qualitatively similar picture follows: Sufficiently large stripe energies lead to the emergence of a *magnetization* reversal, i.e., a magnetic π phase shift appears, whose onset, however, occurs at much larger V_0's ($V_0 \simeq 4t$ for $U = +4t$).

Turning back to the attractive case, to characterize the nature of the charge pattern more precisely, Fig. 3(a) shows the density-density correlation function $c(\mathbf{r} = (x, 0))$ between sites running immediately parallel to the charge stripe. These correlations exhibit an interesting nonmonotonicity with V_0. As might be expected, the oscillating CDW pattern is most robust at $V_0 = 0$ when one has a pristine half-filled lattice. For weak stripe potentials $V_0 = 0.5, 1.0$, there is only short-range order, and $c(\mathbf{r} = (4,0)) \sim 0$. However, as V_0 is further increased, CDW order is recovered. For $V_0 = 3$, $c(\mathbf{r} = (4,0))$ is nearly as large as its $V_0 = 0$ value. Figure 3(b) emphasizes this behavior by showing $c(\mathbf{r} = (4,0))$ as a function of V_0. As a comparison, we also show $c(\mathbf{r} = (4,0))$ along the middle line in the domain as a function of V_0.

The preceding results are for a coupling $U = -4t$ which is one-half the noninteracting bandwidth. The low-temperature spin and charge correlations of the Hubbard Hamiltonian are usually strongest at somewhat larger interaction strengths. In

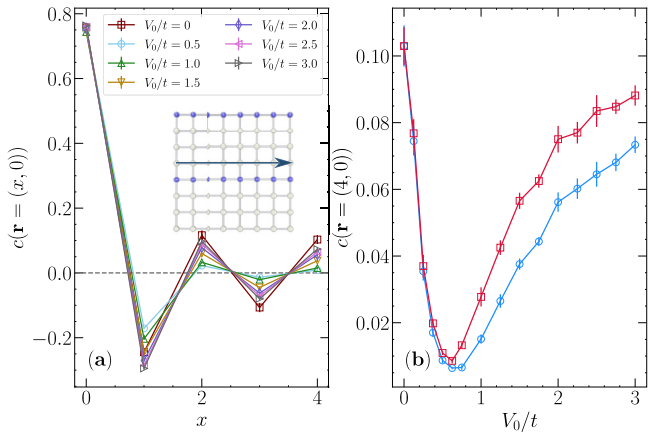

FIG. 3. (a) Density-density correlations $c(\mathbf{r} = (x, 0))$ on a row parallel to, and immediately neighboring, the stripe, as indicated in the lattice of the inset. Results for different values of the stripe strength V_0 are shown. (b) Density-density correlations $c(\mathbf{r} = (4, 0))$ on a row parallel to the stripe, for both immediately neighboring and in the middle of two stripes, as indicated in the lattice of the inset. Results for different values of the stripe strength V_0 are shown. In both panels, the density in the interstripe domains is fixed at $\rho_{\text{dom}} = 1$ by adjusting μ. Here the lattice size is 8×8, the on-site attraction $U = -4t$, and the inverse temperature $\beta t = 10$.

Fig. 4(a) we examine $c(\mathbf{r})$ across a stripe for $U = -6t$. The π phase shift forms at slightly smaller values of V_0. A compilation of the critical energies V_0 that trigger a π phase shift as a function of U is given in Fig. 4(b), showing both the critical V_{0c} and the corresponding fermion occupation on the stripe ρ_{str}. The trend above described is confirmed, that a smaller stripe energy V_0 with systematically larger interactions (in magnitude) is sufficient for the onset of a π phase shift. Even more remarkably, the electronic density at the stripes where the transition occurs is largely U-independent in the range

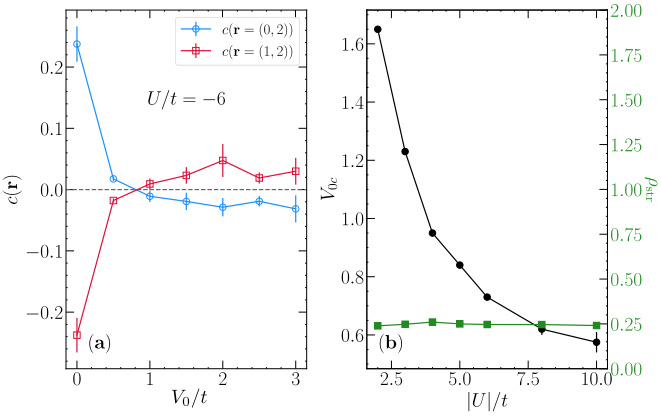

FIG. 4. (a) Similar to Fig. 2(a), but with the interaction strength increased to $U = -6t$. The formation of π phase shift occurs at a slightly smaller stripe potential. (b) Compilation of the critical values V_{0c} where the π phase shift appears with different interaction strengths, and the corresponding electron density on the stripe ρ_{str}. The inverse temperature is set at $\beta t = 10$.

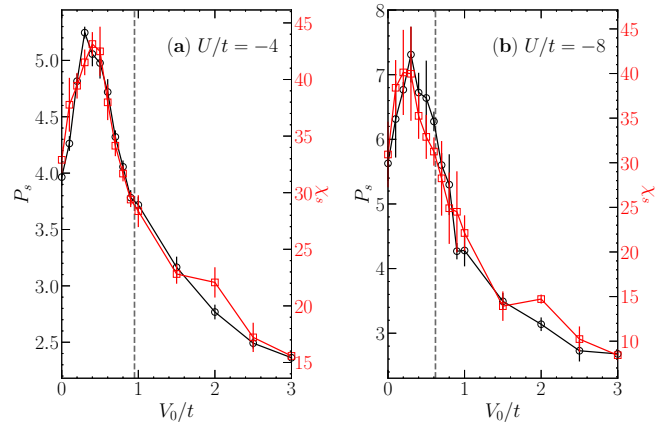

FIG. 5. The s-wave pairing structure factor P_s (left y axes) as a function of V_0 and the corresponding pair susceptibility χ_s (right y axes) for $\rho_{\text{dom}} = 1$, in an 8×8 lattice with $U/t = -4$ (a) and -8 (b). Apart from the very different scales, the two quantities qualitatively follow each other. Vertical dashed lines give the critical stripe strength for π phase shift formation $V_{0c}(U)$. The inverse temperature $\beta t = 10$.

investigated, pinned at filling $\rho_{\text{str}} = 0.25$. This corresponds to the total density $\rho = 0.8125$ ($\rho_{\text{dom}} = 1$).

In Appendix C we show that these results for the cross-stripe spin correlations are converged in both inverse temperature β and spatial lattice size L.

B. s-wave pairing correlations

We next look at how the s-wave pairing is affected by the stripe strength. We begin with the pair structure factor P_s, focusing, as before, on fermionic "domain" occupation $\rho_{\text{dom}} = 1$. Figure 5 shows the dependence of P_s on V_0. Initially (small V_0), the presence of an extrinsic density modulation results in enhanced s-wave pairing. This increase exists roughly up to the value of $V_0 = V_{0c}(U)$ where the charge π phase shift is formed. Subsequently, a further increase in the stripe strength is detrimental to the pairing. This behavior is consistent with trends at different values of the interaction U [see Figs. 5(a) and 5(b)], but is less clear in situations where the π phase shift is not robustly observed (see Appendix D). We conclude that while the density modulation associated with stripes can initially have a positive impact on pairing, it appears that, for the model we study, the subsequent π phase shift does not. It is possible that the complete reversal of the CDW "glue" inhibits the motion of a pair across the stripe. While this observation is of interest to the model under investigation, it is of course not known whether it also applies to the repulsive model, and the associated magnetic sublattice reversal. Although it is not our intent here to model the cuprate superconductors, we note that it is still under debate, in the repulsive Hubbard model, whether d-wave pairing correlations are promoted or inhibited by the stripes [15,52,53]. The appearance of a finite parameter range where pairing correlations are enhanced by inhomogeneity is seen in other contexts, e.g., the plaquette Hubbard model [54,55], and the Hubbard model with modulated hopping in one direction [23].

The pair-field susceptibility,

$$\chi_s = \sum_{\mathbf{r}} \int d\tau \left\langle e^{\tau\hat{\mathcal{H}}} \hat{\Delta}_{\mathbf{i}+\mathbf{r}} e^{-\tau\hat{\mathcal{H}}} \hat{\Delta}_{\mathbf{i}}^{\dagger} \right\rangle, \tag{4}$$

provides a more sensitive measurement of superconductivity (SC), since it also samples over the correlations in imaginary time. χ_s as a function of V_0 for the density $\rho_{\mathrm{dom}} = 1$ is shown (red line) in Fig. 5. The pair structure factor P_s (black line of Fig. 5) and χ_s maintain the same ratio independent of V_0: $\chi_s/P_s \sim \beta$. Indeed, since χ_s includes $\int_0^\beta d\tau$ [see Eq. (4)], a factor of β is the "expected" ratio, assuming there is very little decay in imaginary time. The data of Fig. 5 therefore are indicative of long-range pair correlations in τ.

C. Intertwined order

The preceding results suggest that in this model pairing is initially enhanced when charge stripes are introduced, but that the subsequent development of a π phase shift between the CDW domains then rapidly suppresses the SC. This is a nontrivial result. One might intuitively expect that turning on V_0 would promote SC by doping the stripes away from half filling, but the subsequent diminution by the emergence of CDW sublattice reversal does not have an obvious origin.

We can get a more nuanced view of the interplay of the charge patterns and pairing by recalling that, on a bipartite lattice, the Hamiltonian of Eq. (1) with $U < 0$ has a well-known mapping which reverses the sign to $U > 0$. This is accomplished via a partial particle-hole transformation (PHT) on just one of the spin species: $c_{\mathbf{i}\uparrow} \rightarrow (-1)^{\mathbf{i}} c_{\mathbf{i}\uparrow}^{\dagger}$, leaving $c_{\mathbf{i}\downarrow}$ unchanged. Here $(-1)^{\mathbf{i}} = +1$ (-1) on sublattice A (B). The SC correlations in the attractive case map onto AF correlations in the xy plane of the repulsive model, while CDW correlations map onto AF correlations in the z direction of the repulsive model.

Under this PHT, the additional on-site term V_0 and global chemical potential μ couple to the z component of spin $S_{\mathbf{i}}^z = n_{\mathbf{i}\uparrow} - n_{\mathbf{i}\downarrow}$. As has previously been noted [50,51], the full symmetry of the spin correlators of a Heisenberg antiferromagnet is broken in a Zeeman field. B_z will preferentially favor order in the xy plane. Returning to the attractive Hubbard model, we conclude that the V_0 and μ terms are both likely to favor SC over CDW formation, as we indeed observe for $V_0 \lesssim t$. This analysis, while very useful in the $V_0 = 0$ case, does not appear to lend additional insight into why the enhancement of SC is limited to stripes which are not accompanied by a π phase shift.

Finally, note that this familiar mapping of attractive to repulsive Hubbard model does *not* allow one to infer stripe formation in the attractive case from existing results for $U > 0$. (A full PHT preserves the sign of U, and instead relates the model at fixed U and V_0 to the model at the same U but reversed $-V_0$.)

IV. CONCLUSIONS

In this paper we have shown that the well-known behavior of the AF spin order across a charge stripe in the repulsive Hubbard model, in which the magnetization of the sublattices on opposite sides of a stripe is interchanged, also occurs in CDW order in the attractive Hubbard model. Thus the fact that the magnetic order in the interstripe domain is distinct from the charge pattern of the stripe appears to be irrelevant to the occurrence of a π phase shift. That phenomenon occurs even if the interstripe domain order and stripe physics are both associated with charge degrees of freedom. The physics of the cuprates is often phrased in the context of "intertwined order" in which charge, spin, and pairing correlations are all present and, presumably, influence each others' development [56]. Our paper shows that the π phase shift can occur even in simpler situations with only charge patterns.

A complication with making direct experimental connections to our simulations is that CDW materials tend to be considerably more complex than the cuprates. Whereas many aspects of the physics of the latter (superconductivity, antiferromagnetism, and stripes) are widely believed to be fairly well described by a single orbital model on a square lattice, CDW materials have both more complex lattice geometries and also have multiple relevant orbitals. Nevertheless, there do exist situations where domain reversal, which is qualitatively analogous to what we study here, occurs. Experiments on the transition metal dichalcogenide 1T-TaS_2, for example, reveal (circular) regions of large CDW amplitude separated by intervening low-amplitude areas [57]. Interestingly, there is a well-defined phase shift between the CDWs in adjacent domains, analogous to the structures we demonstrate. A difference is that we have imposed a linear boundary between our domains, whereas the boundaries seen experimentally enclose circular regions. Recent experiments report the control of transitions between commensurate and incommensurate phases electronically [58], complementing tuning via pressure or doping [59–61]. Our π phase shift is a variant of such incommensuration, since it represents an additional, longer wavelength structure superimposed on the rapid site-to-site CDW pattern.

π phase shifts have been observed in several additional contexts in CDW materials, for example in the evolution of the charge pattern across a single unit cell step in the surface of the transition metal kagome metal CsV_3Sb_5 [62]. Another instance is a one-dimensional wire array on a Si surface, where a phase slip defect is associated with a π phase shift in the CDW order [63].

We note that in this work we have exclusively considered stripes which are imposed externally via the potential V_0. We have not considered spontaneous stripe formation, which is a considerably more challenging calculation. In the much-studied repulsive Hubbard model ($U > 0$) case, spontaneous stripes were found early on in inhomogeneous Hartree-Fock calculations [16,17], but are very challenging to see in DQMC [27,28,64] or in quantum Monte Carlo within the dynamical cluster approximation [65].

Although we have found here an *analogous* π phase shift between CDW across a stripe in the attractive Hubbard model, similar to what is known for spin density wave domains in the repulsive case, there is also a potential *difference* between the two situations. DQMC studies of the repulsive Hubbard Hamiltonian [66] found an increase of the stripe strength and the π phase shift keeps enhancing pairing monotonically. In contrast, we find here that the evolution of superconducting correlations with stripe strength is nonmonotonic, and that

when the stripes are sufficiently robust to support a π phase shift, pairing is suppressed. A dynamical cluster approximation treatment [67] of the repulsive case indicates an optimal stripe strength for pairing, but did not examine the π phase shift.

ACKNOWLEDGMENTS

T.Y. was supported by the joint guiding project of Natural Science Foundation of Heilongjiang Province (Grant No. LH2019A011). R.T.S. was supported by the grant DE-SC0014671 funded by the U.S. Department of Energy, Office of Science. R.M. acknowledges support from the National Natural Science Foundation of China (NSFC) Grants No. U1930402, No. 12050410263, No. 12111530010, and No. 11974039.

APPENDICES

These appendices are divided as follows. Appendix A contrasts some of the results to the case with repulsive interactions. Appendices B and C consider the systematic Trotter, finite-temperature, and finite-lattice size errors in our DQMC calculations, showing that they do not affect our conclusions. Appendix D analyzes the charge patterns when μ is not tuned to keep the density in the regions between the stripes at the commensurate filling which is optimal for CDW, $\rho_{\rm dom} = 1$. Finally, Appendix E compares our DQMC results with ED, showing that the qualitative physics is unchanged.

APPENDIX A: THE REPULSIVE CASE: MAGNETIC π PHASE SHIFT

A direct parallel to the results in the main text is given by the repulsive Hubbard model ($U > 0$). These can display a magnetization reversal across a hole-rich region, leading to a *magnetic* π phase shift [66], much like what is observed in certain classes of cuprates with static stripe formation [13,68]. Figure 6 gives the equivalent of Fig. 2, but for $U/t = +4$ instead, and similarly tuning $\rho_{\rm dom} = 1$. Here, we display the spin correlations,

$$c_s(\mathbf{r}) = \langle \hat{S}^z_{\mathbf{i}} \hat{S}^z_{\mathbf{i}+\mathbf{r}} \rangle, \tag{A1}$$

connecting the same [different] sublattice $c_s(\mathbf{r} = (0, 2))$ [$c(\mathbf{r} = (1, 2))$] across a stripe line. Due to the presence of the sign problem, we focus instead on higher temperatures, $\beta t = 5$. Although qualitatively similar, the value of the stripe energy that leads to the AF π phase shift is much larger ($V_{0c} \simeq 4t$) than the one that leads to the density π phase shift ($V_{0c} \simeq t$), both of which with $|U|/t = 4$; yet, the stripe electronic filling at which the magnetization reversal takes place is similar, $\rho_{\rm str} \simeq 0.23$.

The fact that larger V_0 is required to lower the density on a stripe in the repulsive case is due to the presence of a Mott-Slater gap. Single occupancy of sites is energetically preferred, and V_0 must overcome that tendency. Indeed, when thermal and quantum fluctuations are turned off, $T = t = 0$, $V_{0c} = U$ is precisely the critical value for stripe formation. This can be seen by considering a two-site system with V_0 on one site: The configuration $|\uparrow\downarrow\rangle$ with two singly occupied sites has energy $-\frac{U}{4} + (-\frac{U}{4} + V_0)$. The configuration $|\uparrow\downarrow *\rangle$ with a doubly occupied and an empty site has energy $+\frac{U}{4} + \frac{U}{4}$. These become degenerate at $V_{0c} = U$, in agreement with Fig. 6.

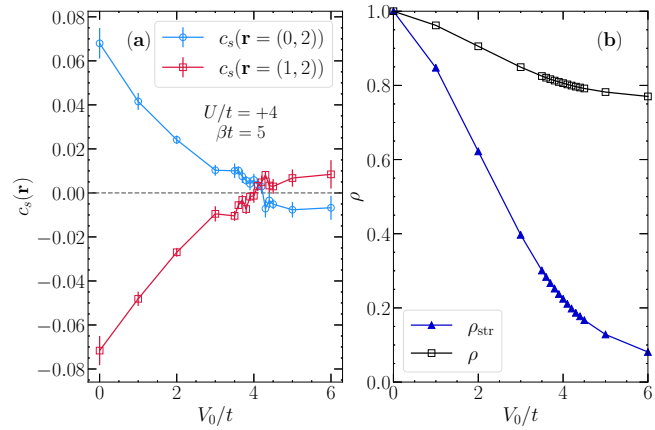

FIG. 6. (a) Spin-spin correlators $c_s(\mathbf{r} = (0, 2))$ and $c_s(\mathbf{r} = (1, 2))$, as functions of stripe strength V_0 for the *repulsive* Hubbard model. *Magnetic* π phase shifts are formed at $V_0 \sim 4t$, where the reversal in sign of the spin correlation functions takes place. (b) The total electron density ρ and the density on the stripe $\rho_{\rm str}$, as functions of stripe strength V_0. As in Fig. 2, the off-stripe electron density, $\rho_{\rm dom}$, is fixed to be 1 by adjusting the global chemical potential μ. Here the lattice size is 8×8, the on-site repulsive interaction is $U = +4t$, and the inverse temperature $\beta t = 5$.

Meanwhile, for the attractive case, double occupation is already favored (on alternating sites). A potential V_0 on a linear set of sites needs only to overcome the charge alternation, an energy scale $\sim 4t^2/U$. This suggests $V_{0c} \sim t$, again, in rough agreement with Fig. 2. In any case, the difference between the values of V_{0c} stresses that the two models are *not* connected by PHT.

APPENDIX B: TROTTER ERRORS

In Fig. 7, we recompute the results for $c(\mathbf{r})$ of Fig. 2 at a smaller $\Delta\tau = 0.0625$. The values are not significantly shifted, and conclusions of the main text are unaltered.

APPENDIX C: FINITE-TEMPERATURE AND FINITE-SIZE EFFECTS

Here we explore the robustness of our results to lowering the temperature further and to increasing the lattice size. Figure 8(a) compares the results for the density correlations across a stripe of Fig. 2(a) (at $\beta t = 10$) with DQMC simulations at $\beta t = 20$. The π phase shift is still observed, and occurs at the same $V_{0c} \sim t$.

To quantify finite-size effects, we increase the lattice size to 12×12, leaving the other parameters unchanged. The π phase shift is still observed, as shown in Fig. 8(b). There is some reduction in the density correlations in going from 8×8 to 12×12 at large V_0. However, the 16×16 lattice results lie on top of those for 12×12, indicating convergence to a nonzero π phase shifted value in the thermodynamic limit.

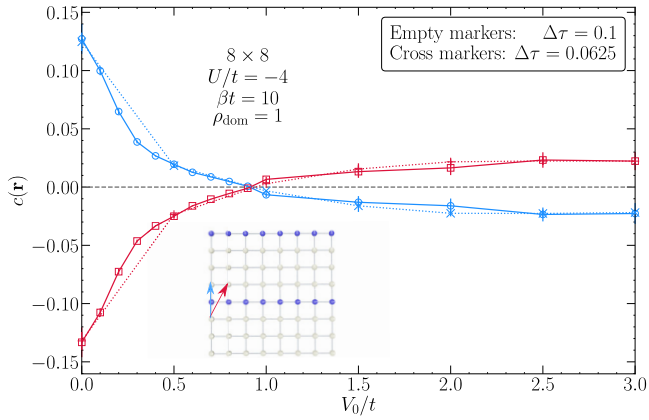

FIG. 7. Density-density correlators $c(\mathbf{r} = (0, 2))$ (blue symbols, and blue arrow in the inset) and $c(\mathbf{r} = (1, 2))$ (red markers, and red arrow in the inset), as functions of stripe strength V_0, for two different imaginary time discretizations $\Delta\tau = 0.1$ (empty markers), the value presented in the main text, and $\Delta\tau = 0.0625$ (cross markers). The results are the same to within the statistical error bars.

APPENDIX D: RESULTS FOR GENERAL $\rho_{\rm dom}$

In Fig. 9(a), we show two density-density correlations traversing the stripe $c(\mathbf{r} = (1, 2))$ and $c(\mathbf{r} = (0, 2))$ for simulations in which μ is not tuned to keep $\rho_{\rm dom} = 1$ but instead the total density $\rho = 1$. Since $\rho = \frac{1}{4}\rho_{\rm str} + \frac{3}{4}\rho_{\rm dom}$ and $\rho_{\rm str} \to 0$ as V_0 becomes large, the density in the interstripe domains interpolates between $\rho_{\rm dom} = 1$ and $\rho_{\rm dom} = \frac{4}{3}$ as V_0 goes from $V_0 = 0$ to $V_0 = \infty$. This is seen in Fig. 9(b). Although $c(\mathbf{r} = (0, 2))$ initially decreases from its positive value at $V_0 = 0$, it recovers and always remains positive. There is no clear signature of π phase shift.

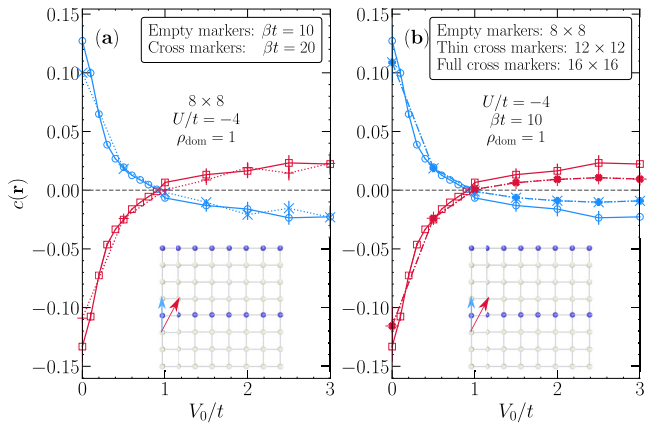

FIG. 8. (a) Density-density correlations $c(\mathbf{r} = (0, 2))$ (blue markers, and blue arrow in the inset) and $c(\mathbf{r} = (1, 2))$ (red markers, and red arrow in the inset), as functions of stripe strength V_0, for two different temperatures $\beta = 10$ (empty markers), the value presented in the main text, and $\beta = 20$ (cross markers) for an 8×8 lattice. The results are the same to within the statistical error bars. (b) Same correlations as functions of stripe strength V_0, but now for three different lattice sizes 8×8 (empty markers), 12×12 (thin cross markers), and 16×16 (full cross markers) at $\beta t = 10$. Data parameters in both panels are $U/t = -4$ and $\rho_{\rm dom} = 1$.

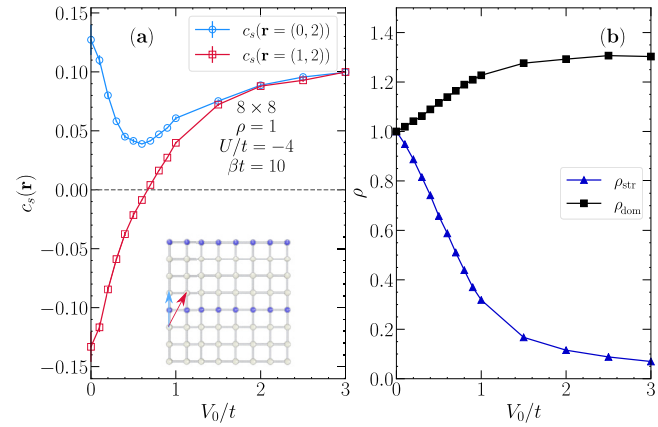

FIG. 9. (a) Similar to Fig. 2(a), but with the *total* electron density ρ fixed to be 1. Although $c(\mathbf{r} = (1, 2))$ exhibits a sign change, $c(\mathbf{r} = (0, 2))$ does not. When the interstripe domains are not pinned at half filling, complete sublattice reversal across a stripe does not occur. (b) The electron density on and off the stripe, as functions of stripe strength V_0, with the total electron density fixed to be 1, and for parameters listed in the figure.

We next performed QMC calculations fixing the total electron density to be 0.75, as shown in Fig. 10(a). We find that, with the increase of V_0, $c(\mathbf{r} = (0, 2))$ goes from positive to negative values as should occur for a π phase shift. Meanwhile $c(\mathbf{r} = (1, 2))$ *begins* already at $V_0 = 0$ with a positive value appropriate to a π phase shift, and remains so as V_0 grows. Thus at large V_0 both correlation functions are consistent with sublattice reversal. The corresponding densities are shown in Fig. 10(b).

In Fig. 11, we show the s-wave pairing structure factor P_s and the s-wave pairing susceptibility χ_s, separately, as functions of V_0. The two panels are similar to Fig. 5, but for $\rho = 1$ and $\rho = 0.75$. For $\rho = 1$ there are peaks in P_s and χ_s similar to those occurring for fixed $\rho_{\rm dom} = 1$. However $\rho = 0.75$ shows no enhancement of SC with the imposition of stripes.

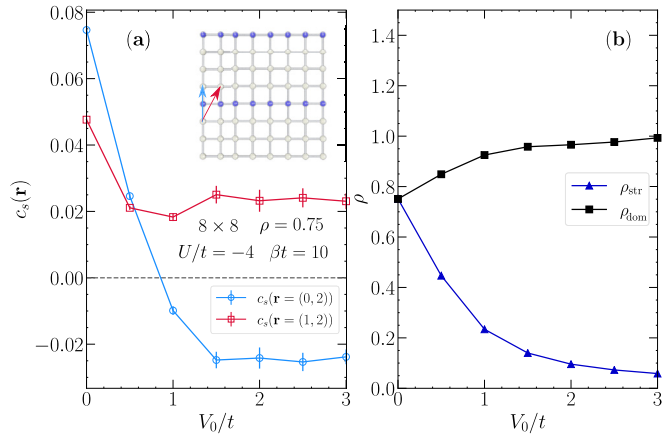

FIG. 10. Same as Fig. 9 but with the total electron density fixed to be 0.75, and for the parameters listed in the figure.

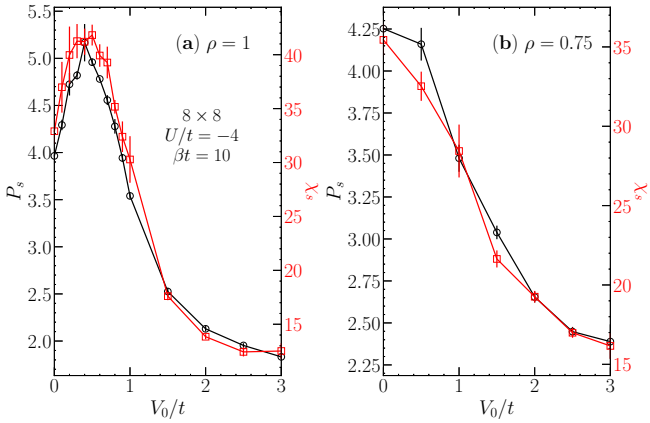

FIG. 11. The s-wave pairing structure factor P_s, left axis (pairing susceptibility χ_s, right axis), as a function of V_0, similar to Fig. 5, but for $\rho = 1$ (a) and $\rho = 0.75$ (b).

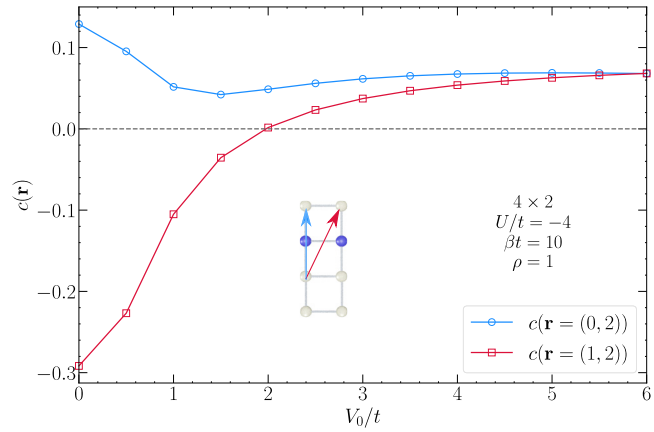

FIG. 12. ED results of the density-density correlator $c(\mathbf{r} = (0, 2))$ (blue circles, and blue arrow in the inset) and $c(\mathbf{r} = (1, 2))$ (red squares, and red arrow in the inset), as functions of stripe strength V_0. The total electron density is fixed to be 1.

APPENDIX E: EXACT DIAGONALIZATION RESULTS

As a complement to the QMC data investigated, we also performed ED calculations on a 2×4 lattice, with the total electron density fixed to be 1, as shown in Fig. 12. The density correlators $c(\mathbf{r} = (0, 2))$ and $c(\mathbf{r} = (1, 2))$ behave in a qualitatively similar way to the QMC data in Fig. 9(a) of Appendix D.

[1] E. Dagotto, Complexity in strongly correlated electronic systems, Science **309**, 257 (2005).

[2] K. Dörr, Ferromagnetic manganites: Spin-polarized conduction versus competing interactions, J. Phys. D **39**, R125 (2006).

[3] W. Eerenstein, N. Mathur, and J. F. Scott, Multiferroic and magnetoelectric materials, Nature (London) **442**, 759 (2006).

[4] C. Israel, M. J. Calderon, and N. D. Mathur, The current spin on manganites, Mater. Today **10**, 24 (2007).

[5] H. Zhang, Y. Zhang, R. Li, J. Yu, W. Dong, C. Chen, K. Wang, X. Tang, and J. Chen, Room temperature hidden state in a manganite observed by time-resolved x-ray diffraction, npj Quantum Mater. **4**, 1 (2019).

[6] N. Doiron-Leyraud, C. Proust, D. LeBoeuf, J. Levallois, J.-B. Bonnemaison, R. Liang, D. Bonn, W. Hardy, and L. Taillefer, Quantum oscillations and the Fermi surface in an underdoped high-T_c superconductor, Nature (London) **447**, 565 (2007).

[7] T. Wu, H. Mayaffre, S. Krämer, M. Horvatić, C. Berthier, W. Hardy, R. Liang, D. Bonn, and M.-H. Julien, Magnetic-field-induced charge-stripe order in the high-temperature superconductor $YBa_2Cu_3O_{7+y}$, Nature (London) **477**, 191 (2011).

[8] T. Wu, H. Mayaffre, S. Krämer, M. Horvatić, C. Berthier, W. Hardy, R. Liang, D. Bonn, and M.-H. Julien, Incipient charge order observed by NMR in the normal state of $YBa_2Cu_3O_{7+y}$, Nat. Commun. **6**, 6438 (2015).

[9] G. Ghiringhelli, M. Le Tacon, M. Minola, S. Blanco-Canosa, C. Mazzoli, N. Brookes, G. De Luca, A. Frano, D. Hawthorn, F. He *et al.*, Long-range incommensurate charge fluctuations in $(Y, Nd)Ba_2Cu_3O_{6+x}$, Science **337**, 821 (2012).

[10] J. Chang, E. Blackburn, A. Holmes, N. B. Christensen, J. Larsen, J. Mesot, R. Liang, D. Bonn, W. Hardy, A. Watenphul *et al.*, Direct observation of competition between superconductivity and charge density wave order in $YBa_2Cu_3O_{6.67}$, Nat. Phys. **8**, 871 (2012).

[11] R. Comin and A. Damascelli, Resonant x-ray scattering studies of charge order in cuprates, Annu. Rev. Condens. Matter Phys. **7**, 369 (2016).

[12] J. Hoffman, E. W. Hudson, K. Lang, V. Madhavan, H. Eisaki, S. Uchida, and J. Davis, A four unit cell periodic pattern of quasiparticle states surrounding vortex cores in $Bi_2Sr_2CaCu_2O_{8+\delta}$, Science **295**, 466 (2002).

[13] J. Tranquada, B. Sternlieb, J. Axe, Y. Nakamura, and S. Uchida, Evidence for stripe correlations of spins and holes in copper oxide superconductors, Nature (London) **375**, 561 (1995).

[14] M.-H. Julien, Magnetic fields make waves in cuprates, Science **350**, 914 (2015).

[15] B.-X. Zheng, C.-M. Chung, P. Corboz, G. Ehlers, M.-P. Qin, R. M. Noack, H. Shi, S. R. White, S. Zhang, and G. K.-L. Chan, Stripe order in the underdoped region of the two-dimensional Hubbard model, Science **358**, 1155 (2017).

[16] J. Zaanen and O. Gunnarsson, Charged magnetic domain lines and the magnetism of high-T_c oxides, Phys. Rev. B **40**, 7391 (1989).

[17] D. Poilblanc and T. M. Rice, Charged solitons in the Hartree-Fock approximation to the large-U Hubbard model, Phys. Rev. B **39**, 9749 (1989).

[18] M. Kato, K. Machida, H. Nakanishi, and M. Fujita, Soliton lattice modulation of incommensurate spin density wave in two dimensional Hubbard model: A mean field study, J. Phys. Soc. Jpn. **59**, 1047 (1990).

[19] H. Yamase, A. Eberlein, and W. Metzner, Coexistence of Incommensurate Magnetism and Superconductivity in the Two-Dimensional Hubbard Model, Phys. Rev. Lett. **116**, 096402 (2016).

[20] S. R. White and D. J. Scalapino, Density Matrix Renormalization Group Study of the Striped Phase in the 2D *t*-*J* Model, Phys. Rev. Lett. **80**, 1272 (1998).

[21] S. R. White and D. J. Scalapino, Stripes on a 6-Leg Hubbard Ladder, Phys. Rev. Lett. **91**, 136403 (2003).

[22] G. Hager, G. Wellein, E. Jeckelmann, and H. Fehske, Stripe formation in doped Hubbard ladders, Phys. Rev. B **71**, 075108 (2005).

[23] H.-C. Jiang and S. A. Kivelson, Stripe order enhanced superconductivity in the Hubbard model, Proc. Natl. Acad. Sci. USA **119**, e2109406119 (2021).

[24] M. Fleck, A. I. Lichtenstein, E. Pavarini, and A. M. Oleś, One-Dimensional Metallic Behavior of the Stripe Phase in $La_{2-x}Sr_xCuO_4$, Phys. Rev. Lett. **84**, 4962 (2000).

[25] T. I. Vanhala and P. Törmä, Dynamical mean-field theory study of stripe order and *d*-wave superconductivity in the two-dimensional Hubbard model, Phys. Rev. B **97**, 075112 (2018).

[26] C.-C. Chang and S. Zhang, Spin and Charge Order in the Doped Hubbard Model: Long-Wavelength Collective Modes, Phys. Rev. Lett. **104**, 116402 (2010).

[27] E. W. Huang, C. B. Mendl, S. Liu, S. Johnston, H.-C. Jiang, B. Moritz, and T. P. Devereaux, Numerical evidence of fluctuating stripes in the normal state of high-T_c cuprate superconductors, Science **358**, 1161 (2017).

[28] E. W. Huang, C. B. Mendl, H.-C. Jiang, B. Moritz, and T. P. Devereaux, Stripe order from the perspective of the Hubbard model, npj Quantum Mater. **3**, 1 (2018).

[29] M. P. Qin, C. M. Chung, H. Shi, E. Vitali, C. Hubig, U. Schollwöck, S. R. White, and S. W. Zhang, Absence of Superconductivity in the Pure Two-Dimensional Hubbard Model, Phys. Rev. X **10**, 031016 (2020).

[30] P. Corboz, T. M. Rice, and M. Troyer, Competing States in the *t*-*J* Model: Uniform *d*-Wave State versus Stripe State, Phys. Rev. Lett. **113**, 046402 (2014).

[31] B.-X. Zheng and G. K.-L. Chan, Ground-state phase diagram of the square lattice Hubbard model from density matrix embedding theory, Phys. Rev. B **93**, 035126 (2016).

[32] M. Qin, T. Schäfer, S. Andergassen, P. Corboz, and E. Gull, The Hubbard model: A computational perspective, Annu. Rev. Condens. Matter Phys. **13**, 275 (2022).

[33] G. Campi, A. Bianconi, N. Poccia, G. Bianconi, L. Barba, G. Arrighetti, D. Innocenti, J. Karpinski, N. D. Zhigadlo, S. M. Kazakov, M. Burghammer, M. v. Zimmermann, M. Sprung, and A. Ricci, Inhomogeneity of charge-density-wave order and quenched disorder in a high-T_c superconductor, Nature (London) **525**, 359 (2015).

[34] H. Miao, J. Lorenzana, G. Seibold, Y. Y. Peng, A. Amorese, F. Yakhou-Harris, K. Kummer, N. B. Brookes, R. M. Konik, V. Thampy, G. D. Gu, G. Ghiringhelli, L. Braicovich, and M. P. M. Dean, High-temperature charge density wave correlations in $La_{1.875}Ba_{0.125}CuO_4$ without spin-charge locking, Proc. Natl. Acad. Sci. USA **114**, 12430 (2017).

[35] H. Huang, S.-J. Lee, Y. Ikeda, T. Taniguchi, M. Takahama, C.-C. Kao, M. Fujita, and J.-S. Lee, Two-Dimensional Superconducting Fluctuations Associated with Charge-Density-Wave Stripes in $La_{1.87}Sr_{0.13}Cu_{0.99}Fe_{0.01}O_4$, Phys. Rev. Lett. **126**, 167001 (2021).

[36] J.-J. Wen, H. Huang, S.-J. Lee, H. Jang, J. Knight, Y. S. Lee, M. Fujita, K. M. Suzuki, S. Asano, S. A. Kivelson, C.-C. Kao, and J.-S. Lee, Observation of two types of charge-density-wave orders in superconducting $La_{2-x}Sr_xCuO_4$, Nat. Commun. **10**, 3269 (2019).

[37] X. M. Chen, C. Mazzoli, Y. Cao, V. Thampy, A. M. Barbour, W. Hu, M. Lu, T. A. Assefa, H. Miao, G. Fabbris, G. D. Gu, J. M. Tranquada, M. P. M. Dean, S. B. Wilkins, and I. K. Robinson, Charge density wave memory in a cuprate superconductor, Nat. Commun. **10**, 1435 (2019).

[38] J. Choi, O. Ivashko, E. Blackburn, R. Liang, D. A. Bonn, W. N. Hardy, A. T. Holmes, N. B. Christensen, M. Hücker, S. Gerber, O. Gutowski, U. Rütt, M. v. Zimmermann, E. M. Forgan, S. M. Hayden, and J. Chang, Spatially inhomogeneous competition between superconductivity and the charge density wave in $YBa_2Cu_3O_{6.67}$, Nat. Commun. **11**, 990 (2020).

[39] S. Banerjee, W. A. Atkinson, and A. P. Kampf, Emergent charge order from correlated electron-phonon physics in cuprates, Commun. Phys. **3**, 161 (2020).

[40] Z. Chen, Y. Wang, S. N. Rebec, T. Jia, M. Hashimoto, D. Lu, B. Moritz, R. G. Moore, T. P. Devereaux, and Z.-X. Shen, Anomalously strong near-neighbor attraction in doped 1D cuprate chains, Science **373**, 1235 (2021).

[41] Y. Wang, Z. Chen, T. Shi, B. Moritz, Z.-X. Shen, and T. P. Devereaux, Phonon-Mediated Long-Range Attractive Interaction in One-Dimensional Cuprates, Phys. Rev. Lett. **127**, 197003 (2021).

[42] G. Profeta, M. Calandra, and F. Mauri, Phonon-mediated superconductivity in graphene by lithium deposition, Nat. Phys. **8**, 131 (2012).

[43] S.-L. Yang, J. A. Sobota, C. A. Howard, C. J. Pickard, M. Hashimoto, D. H. Lu, S.-K. Mo, P. S. Kirchmann, and Z.-X. Shen, Superconducting graphene sheets in CaC_6 enabled by phonon-mediated interband interactions, Nat. Commun. **5**, 3493 (2014).

[44] K. C. Rahnejat, C. A. Howard, N. E. Shuttleworth, S. R. Schofield, K. Iwaya, C. F. Hirjibehedin, C. Renner, G. Aeppli, and M. Ellerby, Charge density waves in the graphene sheets of the superconductor CaC_6, Nat. Commun. **2**, 558 (2011).

[45] E. Y. Loh, J. E. Gubernatis, R. Scalettar, S. R. White, D. J. Scalapino, and R. Sugar, Sign problem in the numerical simulation of many-electron systems, Phys. Rev. B **41**, 9301 (1990).

[46] M. Troyer and U.-J. Wiese, Computational Complexity and Fundamental Limitations to Fermionic Quantum Monte Carlo Simulations, Phys. Rev. Lett. **94**, 170201 (2005).

[47] R. Blankenbecler, D. J. Scalapino, and R. L. Sugar, Monte Carlo calculations of coupled boson-fermion systems. I, Phys. Rev. D **24**, 2278 (1981).

[48] S. R. White, D. J. Scalapino, R. L. Sugar, E. Y. Loh, J. E. Gubernatis, and R. T. Scalettar, Numerical study of the two-dimensional Hubbard model, Phys. Rev. B **40**, 506 (1989).

[49] J. E. Hirsch, Discrete Hubbard-Stratonovich transformation for fermion lattice models, Phys. Rev. B **28**, 4059 (1983).

[50] R. Scalettar, N. Bickers, and D. Scalapino, Competition of pairing and Peierls–charge-density-wave correlations in a two-dimensional electron-phonon model, Phys. Rev. B **40**, 197 (1989).

[51] A. Moreo and D. J. Scalapino, Two-Dimensional Negative-*U* Hubbard Model, Phys. Rev. Lett. **66**, 946 (1991).

[52] D. Scalapino and S. White, Numerical results for the Hubbard model: Implications for the high-T_c pairing mechanism, Found. Phys. **31**, 27 (2001).

[53] B. Ponsioen, S. S. Chung, and P. Corboz, Period 4 stripe in the extended two-dimensional Hubbard model, Phys. Rev. B **100**, 195141 (2019).

[54] W.-F. Tsai and S. A. Kivelson, Superconductivity in inhomogeneous Hubbard models, Phys. Rev. B **73**, 214510 (2006).

[55] T. Ying, R. Mondaini, X. D. Sun, T. Paiva, R. M. Fye, and R. T. Scalettar, Determinant quantum Monte Carlo study of d-wave pairing in the plaquette Hubbard Hamiltonian, Phys. Rev. B **90**, 075121 (2014).

[56] E. Fradkin, S. A. Kivelson, and J. M. Tranquada, *Colloquium*: Theory of intertwined orders in high-temperature superconductors, Rev. Mod. Phys. **87**, 457 (2015).

[57] X. L. Wu and C. M. Lieber, Hexagonal domain-like charge density wave phase of TaS_2 determined by scanning tunneling microscopy, Science **243**, 1703 (1989).

[58] A. W. Tsen, R. Hovden, D. Wang, Y. D. Kim, J. Okamoto, K. A. Spoth, Y. Liu, W. Lu, Y. Sun, J. C. Hone, L. F. Kourkoutis, P. Kim, and A. N. Pasupathy, Structure and control of charge density waves in two-dimensional $1T - TaS_2$, Proc. Natl. Acad. Sci. USA **112**, 15054 (2015).

[59] L. J. Li, W. J. Lu, X. D. Zhu, L. S. Ling, Z. Qu, and Y. P. Sun, Fe-doping–induced superconductivity in the charge-density-wave system $1T - TaS_2$, Europhys. Lett. **97**, 67005 (2012).

[60] Y. Liu, R. Ang, W. J. Lu, W. H. Song, L. J. Li, and Y. P. Sun, Superconductivity induced by Se-doping in layered charge-density-wave system $1T - TaS_{2-x}Se_x$, Appl. Phys. Lett. **102**, 192602 (2013).

[61] B. Sipos, A. F. Kusmartseva, A. Akrap, H. Berger, L. Forró, and E. Tutiš, From Mott state to superconductivity in $1T - TaS_2$, Nat. Mater. **7**, 960 (2008).

[62] Z. Liang, X. Hou, F. Zhang, W. Ma, P. Wu, Z. Zhang, F. Yu, J.-J. Ying, K. Jiang, L. Shan, Z. Wang, and X.-H. Chen, Three-Dimensional Charge Density Wave and Surface-Dependent Vortex-Core States in a Kagome Superconductor CsV_3Sb_5, Phys. Rev. X **11**, 031026 (2021).

[63] T.-H. Kim and H. W. Yeom, Topological Solitons versus Nonsolitonic Phase Defects in a Quasi-One-Dimensional Charge-Density Wave, Phys. Rev. Lett. **109**, 246802 (2012).

[64] E. W. Huang, T. Liu, W. O. Wang, H.-C. Jiang, P. Mai, T. A. Maier, S. Johnston, B. Moritz, and T. P. Devereaux, Fluctuating intertwined stripes in the strange metal regime of the Hubbard model, arXiv:2202.08845.

[65] P. Mai, S. Karakuzu, G. Balduzzi, S. Johnston, and T. A. Maier, Intertwined spin, charge, and pair correlations in the two-dimensional Hubbard model in the thermodynamic limit, Proc. Natl. Acad. Sci. USA **119**, e2112806119 (2022).

[66] R. Mondaini, T. Ying, T. Paiva, and R. T. Scalettar, Determinant quantum Monte Carlo study of the enhancement of d-wave pairing by charge inhomogeneity, Phys. Rev. B **86**, 184506 (2012).

[67] T. A. Maier, G. Alvarez, M. Summers, and T. C. Schulthess, Dynamic Cluster Quantum Monte Carlo Simulations of a Two-Dimensional Hubbard Model with Stripelike Charge-Density-Wave Modulations: Interplay between Inhomogeneities and the Superconducting State, Phys. Rev. Lett. **104**, 247001 (2010).

[68] J. M. Tranquada, H. Woo, T. G. Perring, H. Goka, G. D. Gu, G. Xu, M. Fujita, and K. Yamada, Quantum magnetic excitations from stripes in copper oxide superconductors, Nature (London) **429**, 534 (2004).